

Assessing posttraumatic time interval in human dry bone

H. H. DE BOER,^{a*} A. E. VAN DER MERWE,^b S. HAMMER,^c M. STEYN^d AND G. J. R. MAAT^a

^a Leiden University Medical Center, Barge's Anthropologica, Dept. of Anatomy, Leiden, Netherlands

^b Amsterdam Medical Center, Dept. of Anatomy, Embryology and Physiology, Amsterdam, Netherlands

^c Leiden University Medical Center, Dept. of Radiology, Leiden, Netherlands

^d University of Pretoria, Forensic Anthropologic Research Center, Dept. of Anatomy, Pretoria, South Africa

Abstract

The post-traumatic status of antemortem fractures in human dry bone remains is currently defined as being either 'healing' or 'healed'. However, detailed 'dating' of the related post-traumatic time interval would be desirable, since it would aid in assessing individual medical status and care at the time of death. Within forensic pathology practice, fresh tissue healing phases are routinely used as an intrinsic parameter for the length of the post-traumatic time interval. Unfortunately, the direct application of such a method is hampered when applied to dry bone skeletal material.

This study explores the possibility of applying a fracture dating system, drawn forth from the traditional forensic pathology method, on dry bone remains. More specifically, the aim is to establish the extent to which various histo-morphological features indicative of specific time intervals of healing are consistently detectable. Human dry bones with fractures and amputations in various phases of healing were studied.

Results show that the complementary use of radiological and histological investigation techniques improves the differentiation between various healing phases and thus allow for a more detailed dating of lesions. For future use, healing features that have proven to be consistently detectable and their related post traumatic time intervals are listed. The system aids in demarcating a considerably more "narrow" post-traumatic time interval than usual.

Introduction

It is generally agreed upon that studying trauma in human remains can yield interesting individual, cultural and environmental information (Krogman and İşcan, 1986; Ortner, 2003, Auferheide and Rodríguez-Martin, 1998). Indeed, a large pool of literature exists describing and interpreting gross anatomical traumatic lesions observed in skeletons such as fractures, amputations and dislocations (e.g., Berryman and Haun, 1996, Grauer and Roberts, 1996; Mays, 1996; Lovell, 1997; Alvrus, 1999; Galloway, 1999; Judd and Roberts, 1999; Nakai *et al.*, 2001; Anderson, 2002; Holt *et al.*, 2002; Mitchell, 2006; Djuric *et al.*, 2006; Lovell, 2008; Van der Merwe *et al.*, 2009; Redfern, 2009).

Notwithstanding its acceptance, investigating traumatic lesions in dry bone tissue is still challenging, since palaeopathologists, and sometimes forensic pathologists and anthropologists, are confronted with the investigation of material that lacks soft tissue (Uberlaker and Adams, 1995; Grauer and Roberts, 1996; Lovell, 1997; Sauer, 1998; Rodríguez-Martin, 2006; Ortner 2003). Traditionally, the moment that lesions are inflicted is defined as being either 'antemortem' (prior to death), perimortem (occurring around the time of death) or 'postmortem' (after death). Antemortem lesions are defined by the presence of healing features (e.g. callus formation), whereas postmortem lesions are defined by the lack of any healing features. For postmortem lesions that occurred

during excavation, the colour difference between fracture surface and periosteal surface may also aid in identifying postmortem lesions (Van der Merwe *et al.* 2009). Perimortem lesions are generally those that cannot be reliably assigned to either the ante- or postmortem group. A more detailed discussion of the differentiation between ante- peri- and postmortem lesions is beyond the scope of this publication, but can be found in various comprehensive publications (e.g. Quatrehomme and Iscan, 1997; Wheatley, 2008; Wieberg and Wescott, 2008).

Describing lesions as being either, antemortem, perimortem or postmortem has severe limitations as it gives no estimation of the length of the time period between the moment the traumatic insult occurred and the time of death (the posttraumatic interval). Usually the status of antemortem lesions is expressed as being 'healing' or 'healed' (see for instance Brickley, 2006). However, a more detailed temporal specification of antemortem time would be desirable, since a more precise 'dating' would aid palaeopathologists and forensic anthropologists in interpreting facets such as medical status and medical care at the time of death. More specific information on differences in the timing of multiple injuries in a specific individual may also be essential in evaluating evidence for child abuse and torture (e.g., Maat 2008). Also it would assist in determining the sequence of multiple traumata observed in a single individual. The latter could especially be an addition to the growing body of research that studies the occurrence of trauma recidivism (e.g. Judd, 2002; Martin *et al.*, 2010).

Theory and practice of dating traumatic lesions

In forensic pathological investigations, estimation of the posttraumatic interval is usually done by analyzing the local soft tissue response (healing), since healing is supposed to be an intrinsic and reliable time indicator (e.g. Oehmichen, 2004). Although in forensic pathology practice dating is mostly applied to soft tissue lesions (e.g. cutaneous wounds), the principle can also be utilized for bone tissue injuries, since bone tissue response also follows a strict time dependant developmental sequence irrespective of complex variables such as the type of lesion, location, age at death and health status (Todd and Iler 1927, Frost 1989a, Frost 1989b, Tosounidis *et al.*, 2009, Vigorita 2009).

The usefulness of healing as an indicator of posttraumatic survival time was, for instance, illustrated in an investigation of war crimes. Following an extensive literature review on fracture healing, a time table was constructed and applied that linked the elapsed time after bone tissue injury to radiographic and histological healing features (Maat, 2008). The approach proved to be adequate for cases regarding adult and paediatric individuals (Maat and Huls, 2010).

Despite the fact that the approach was designed for fracture dating, it should also be suitable for amputations, since stages and timing of bone healing are supposed to be similar (Barber 1930). Comparisons between Maat's timetable (2008), based on a literature review of microscopic and radiologic observations, and the work by Barber remains (1929, 1930, 1934), based on gross anatomical and radiological observations in macerated, supports this statement.

Application in palaeopathology and forensic anthropology

It goes without saying that forensic pathological trauma dating has great potential for implementation in palaeopathology. This was for instance demonstrated by Mays (1996)

who applied Barber's gross anatomical approach in a case study regarding healed amputations (Barber, 1929, 1930, 1934; Todd and Barber 1934). Recently, Cattaneo *et al.* (2010) also showed that useful histological markers for the dating of traumatic lesions were even traceable in macerated bone. However, macerated bone material, like fresh forensic material, is usually better preserved than archaeological dry bone material. It therefore allows for 'better' analysis. As a result, the consistency in the detectability of healing features as used in the approaches of Maat (2008) and Barber (1929, 1930, 1934) are still left to be tested in case of dry bone material.

This study will therefore specifically attempt to: (1) evaluate which features (as described by Barber (1929, 1930, 1934)) and Maat (2008) are adequately assessable in traumatic lesions in dry bone material, and (2) to determine to what extent they allow for estimation of the 'age' of an injury.

Materials and Methods

Material

Dry bone specimens from various collections were assembled in order to ensure a sufficiently large sample for investigation. Only traumata from presumably healthy individuals were included. Because of the destructive nature of histological methods we were not permitted to sample cranial bone material. Therefore only post-cranial material was included in the study. There is however no indication that the healing process and its timing would be different in cranial bones from that in post-cranial ones (Vigorita, 1999; Frost 1989a, 1989b).

A total of 22 specimen with fractures and nine amputations in various phases of healing were included in this study. They were excised from 21 individuals. Twelve fractures and seven amputations were obtained from the Gladstone skeletal collection from Kimberley, South Africa (Van der Merwe *et al.*, 2009). One fracture originated from a 17th century Dutch male whaler exhumed on Spitsbergen, Norway (Maat, 1981), and two fractures from a 19th century population from Bloemendaal, The Netherlands. The sample was further extended with six fractures and one amputation from the dissection hall collection of the Leiden University Medical Centre (LUMC). Three intentionally sawn/broken specimens from the Bloemendaal collection were used as controls.

Throughout our assemblage, wherever possible, a (contra lateral) control sample was included for comparison of bone density and histological architecture. General information on the studied bone material is listed in Table 1.

Methods

All lesions were photographed and studied gross anatomically, to define whether they are either ante-, peri- or post-mortem. For this, we used standard anthropological methods (Van der Merwe *et al.*, 2009). Subsequently, conventional plain radiographs in an anterior-posterior and a medio-lateral direction were taken. The lesion plus a representative length of unaffected bone was imaged together with its contra lateral control specimen (whenever available). To prevent bias by specimen recognition, each image was anonymized by random numbering.

After radiological imaging, histology samples, so called 'thick slices', were excised from the centre of each lesion and its control (i.e. perpendicular to the fracture/amputation

Table 1. Skeletal material.

	Individual No.^a	Origin	Bone	Gross anatomica dating^b	Preservation phase^c
<i>Fractures</i>	N74.5	Kimberly, SA	Hu	Antemortem	1
	N38.1	Kimberly, SA	Ri	Perimortem	1
	N38.2	Kimberly, SA	Fe	Antemortem	1
	N38.2	Kimberly, SA	Ti	Antemortem	1
	N38.2	Kimberly, SA	3 th MCP	Antemortem	1
	N38.3	Kimberly, SA	Ra	Antemortem	1
	N74.4	Kimberly, SA	Ul	Antemortem	1
	S2.3	Kimberly, SA	Fe	Perimortem	2
	S2.3	Kimberly, SA	Ra	Antemortem	2
	S2.9	Kimberly, SA	8 th Ri	Antemortem	1
	S3.5	Kimberly, SA	Fe	Perimortem	2
	Sk. 1	Unknown, NL	Fi	Antemortem	1
	Sk. 2	Unknown, NL	Ti	Antemortem	1
	Sk. 2	Unknown, NL	Fi	Antemortem	1
	Sk. 4	Unknown, NL	Fe	Antemortem	1
	Sk. 5	Unknown, NL	Hu	Antemortem	1
	Sk. 5	Unknown, NL	Ra	Antemortem	1
	541	Spitsbergen, NO	Fe	Antemortem	1
	1033	Bloemendaal, NL	Ri	Antemortem	2
	1033	Bloemendaal, NL	Ri	Antemortem	2
H 1	Bloemendaal, NL	St	Postmortem	2	
H 2	Bloemendaal, NL	Fe	Postmortem	2	
<i>Amputations</i>	N34.3	Kimberly, SA	Ti	Antemortem	2
	N38.2	Kimberly, SA	Fe	Perimortem	1
	N8.1	Kimberly, SA	Ti	Antemortem	2
	S2.6	Kimberly, SA	Ti	Antemortem	1
	S2.7	Kimberly, SA	Hu	Perimortem	2
	S2.7	Kimberly, SA	Hu	Antemortem	2
	S2.7	Kimberly, SA	Ra+Ul	Perimortem	2
	Sk. 3	Unknown, NL	Fe	Antemortem	1
	H 2	Bloemendaal, NL	Fe	Postmortem	2

Abbreviations: SA=South Africa; NO=Norway; NL=The Netherlands; Hu=Humerus; Fe=Femur; Ra=Radius; Ul=Ulna; Ri=Rib; Ti=Tibia; Fi=Fibula; MCP=Metacarpal; St=Sternum.

^a Numbering used in prior published articles.

^b According to Van der Merwe et al (2009).

^c According to Gordon and Buikstra (1981).

plane). A new random numbering blinded the identity of these ‘thick slices’. From each thick slice, two thin sections were produced with a minor adaptation according to the method of De Boer *et al.* (2011): i.e., the embedding medium was also used for cover slipping. One of the thin sections remained unstained; the other was stained with haematoxylin to enhance the visibility of tissue architecture. All sections were microscopically investigated using bright- and polarized-light.

By combining the work of Barber (1929, 1930, 1934), Maat (2008; pers. comm.) and Maat and Huls (2010), a table was constructed in which healing features were linked to time intervals (Table 2). Features that are impossible to assess in archaeological material, such as soft tissue changes, were not taken into account. In the few cases in which descriptions given by Maat and Barber did not agree (some minor gross anatomical changes), preference was given to the publication of Maat, since it included a larger quantity of and more recent data. The merged data were then used to develop a multiple choice questionnaire that addressed the consistency in detectability by examiners of each of the designated healing features.

This questionnaire was then used to assess the radiographs and histological sections. By letting 3 examiners assess the images and sections independently, we diminish inter-observer bias to a minimum. In the questionnaire, each healing feature could be marked as: ‘yes’ (the described feature was present), ‘no’ (the described feature was not present), a question mark (the provided image/section did not allow for a conclusive answer), or as ‘NA’ (not applicable). Agreement between the three examiners, and thus consistency in the detection of healing features, was measured by calculating a one way random Intraclass Correlation Coefficient (ICC) for each healing feature for each modality. Prior established categories were used to interpret the ICC. According to Landis and Koch (1977), an ICC greater than 0.6 is considered to reflect substantial agreement between examiners.

Results

In the following text, all healing features will be printed in *italics*. Due to the nature of dry bone tissue, two features of healing described by Maat (*scattered bone spiculae* and *fields of calcified cartilage at sites of callus formation*) were not present in any of our samples.

Furthermore, as expected, healing features were absent in the postmortem control samples included in this study.

Results of radiographic analyses

In analysis of the plain radiographs, several common healing features were detected with substantial interobserver agreement. Agreement on the presence of *clearly visible callus* at the lesion site, both at the *endosteal* and *periosteal* aspect was substantial (ICC 0.756 and 0.770). The examiners also agreed upon the existence of remodeling of endosteal callus making it *indistinguishable from the cancellous bone* (ICC of 0.837). Internal and external callus formation at some distance from the lesion site produced low Intraclass Correlation Coefficients (ICC of 0.345 and 0.343). Also the evaluation of *absorption of the cortical bone adjacent to the lesion* (ICC of 0.275), *more sclerotic lesion margins* (ICC of 0.421), *osteoporosis of the cortex* (ICC of 0.341), the presence of *smoothing of*

Table 2. Healing features and associated posttraumatic time intervals, combined from Barber (1929, 1930, 1934), Maat et al. (2008, 2010) and Maat (pers. comm.).

Category of lesion	Healing feature	Time interval
<i>Common</i>	<ul style="list-style-type: none"> • Frayed bone lamellae at the lesion margins² • Absorption of the cortical bone adjacent to the lesion¹ • First Howship's lacunae at the lesion margins² • Smoothing of the lesion margins^{1,2} • Start of endosteal and periosteal osteogenesis separable from cortex^{1,2} • Periosteal osteogenesis at distance from the fracture site • Clearly visible endosteal callus formation^{1,2} • Aggregation of spiculae into woven bone^{1,2} • Primary bone tissue deposition² • Osteoporosis of the cortex^{1,2} • Margin of the lesion appears more sclerotic¹ • Start of the transition of primary woven bone into secondary lamellar bone² • Cortical 'cutting and closing cones' orientated towards the lesion² • Fields of calcified cartilage at sites of callus formation • Clearly visible periosteal callus^{1,2} • Endosteal callus becomes indistinguishable from the cancellous bone in the marrow cavity^{1,2} • Periosteal callus becomes firmly attached (inseparable) to the cortex^{1,2} 	<p>Before 48 hours</p> <p>After 4-7 days</p> <p>After 4-7 days</p> <p>After 4-7 days</p> <p>After 7 days</p> <p>After 7 days</p> <p>After 10-12 days</p> <p>After 12-20 days</p> <p>After 12-20 days</p> <p>After 12 days</p> <p>After 12-20 days</p> <p>After 14 days</p> <p>After 14-21 days</p> <p>After 14 days</p> <p>After 15 days</p> <p>After 17 days</p> <p>After 6 weeks</p>
<i>Specific for fractures</i>	<ul style="list-style-type: none"> • First scattered bone tissue spiculae between the lesion ends^{1,2} • Union by bridging of the cortical bone discontinuity^{1,2} • Smoothing of the callus outline² • After inadequate immobilization: Pseudoarthrosis development^{1,2} • After adequate immobilization: Quiescent appearance indicating subsided healing^{1,2} 	<p>After 4-7 days</p> <p>After 21-28 days</p> <p>After 2-3 months</p> <p>After 6-9 months</p> <p>After 1-2 years</p>
<i>Specific for amputations</i>	<ul style="list-style-type: none"> • Visibility of cut marks on the amputation surface¹ • Start of 'capping' of the medullary cavity¹ • Complete capping of the medullary cavity¹ 	<p>Less than 13 days</p> <p>After 'not many weeks'</p> <p>After 'several months'</p>

¹ Features visible by plain radiographic analysis.

² Features visible by histological analysis.

lesion margins (ICC of 0.416) and *firm attachment of periosteal callus to the cortex* (ICC of 0.154) did not produce substantial interobserver agreement.

In fractures, examiners agreed upon the detectability of the *smoothing of the callus outline* (ICC of 0.838). High Intraclass Correlation Coefficients were also seen with regard to the *union by bridging of the cortical bone discontinuity*, irrespective of whether this union was constructed by means of primary woven or secondary lamellar bone (ICC of 0.608 and 0.939).

When considering amputations, no differences in observation were seen between examiners regarding *the start of 'capping' of the medullary cavity* with newly formed bone, or the *complete capping of the medullary cavity* (both an ICC of 1.000). In contrast to histological analysis there was no substantial agreement on the detectability of *cut marks on the amputation surface* in radiological analyses.

Results of histological analysis

On a microscopic level, a number of healing features were detected with substantial interobserver agreement, irrespective of the use of histochemical staining. The presence of *frayed bone lamellae at the lesion margins* (ICC of 0.881 and stained 0.763), *smoothing of the lesion margins* (ICC of 0.806 and stained 0.863), and the presence of *clearly visible callus formation* at the lesion site, both *endosteally* (ICC of 0.736 and stained 0.709) and *periosteally* (ICC of 0.912 and stained 1.000) showed substantial agreement. Also, *firm attachment of callus on the periosteal surface* (ICC of 0.900 and stained 0.739) and *quiescent appearance* of the lesion site after healing has concluded (ICC of 1.000 and stained 0.741) were generally agreed upon in both unstained and stained sections. Agreement regarding early indications of *periosteal osteogenesis at distance from the fracture margins* were considered 'borderline' (ICC of 0.678 and stained 0.649). The examiners did not agree convincingly on the detectability of *endosteal osteogenesis* at some distance from the fracture site (ICC of 0.625 and stained 0.393).

Agreement on the detectability of some common healing features (fractures and amputations) was lower in haematoxylin stained sections. In stained sections, agreement was lower on the presence of *Howship's lacunae* (ICC of 0.700 vs. stained 0.575) and *cutting and closing cones* (ICC of 0.965 vs. stained 0.577). Also the final stage of endosteal callus remodeling, when *endosteal callus becomes indistinguishable from the cancellous bone*, was better detectable in unstained sections (ICC of 0.845 vs. stained 0.370). The agreement on detectability of *transition of primary woven bone into secondary lamellar bone* in callus was higher in haematoxylin stained sections, both in endosteally (ICC of 0.491 vs. stained 1.000) and periosteally situated callus (ICC of 0.242 vs. stained 1.000).

In fractures, differences existed in the ICCs between observations done in unstained and stained sections. There was, however, substantial agreement upon the detectability of *union by bridging of the cortical bone discontinuity* by primary woven bone in both unstained and stained sections (ICC of 0.882 and stained 0.629). In contrast, agreement on the presence of *union by bridging of the cortical bone discontinuity* by secondary lamellar bone was reduced in unstained if compared to stained sections (ICC of 0.443 vs. stained 0.764). The *smoothing of callus outline* was inconsistently assessed in

fractures, irrespective of the application of haematoxylin (ICC of 0.510 and stained 0.348).

When considering unstained and stained sections of amputations, features such as the presence of *cut marks* (ICC of 1.000 and 0.825), the *start of 'capping' the medullary cavity* with newly formed bone (both an ICC of 1.000) and eventual *complete 'capping' of the medullary cavity* (ICC of 1.000 and 0.875) were all detected with substantial interobserver agreement.

Table 3. Intraclass Correlation Coefficients of healing features, for microscopic and radiographic analyses.

Healing feature	Unstained histology ICC (95% CI)	Stained histology ¹ ICC (95% CI)	X-ray analysis ICC (95% CI)
Smoothing of the lesion margins	.806 (.629-.917)	.863 (.726-943)	.416 (.125-.693)
Absorption of cortical bone adjacent to the lesion	NA	NA	.275 (.052-.632)
Presence of endosteal callus			
Distant from the lesion site	.652 (.470-.798)	.393 (.178-.608)	.345 (.131-.580)
At the lesion site	.736 (.583-.851)	.709 (.546-.834)	.756 (.611-.863)
Presence of periosteally situated callus			
Distant from the fracture site	.678 (.505-.815)	.649 (.455-.799)	.343 (.126-.568)
At the lesion site	.912 (.848-.953)	1.000 ²	.770 (.629-.871)
Firm attachment of periosteally situated callus.	.900 (.766-.967)	.739 (.484-.902)	.154 (.000-.532)
Local osteoporosis of the cortex	.664 (.484-806)	.706 (.540-.832)	.341 (.116-.574)
Margin of the lesion appears more sclerotic	NA	NA	.421 (.204-632)
Endosteal callus becomes indistinguishable from the cancellous bone in the marrow cavity	.845 (.740-.916)	.370 (152-.590)	.837 (.728-.911)
Features specific for fractures³			
Union by bridging of the cortical bone discontinuity by primary woven bone	.882 (.779-.945)	.629 (.403-.807)	.608 (.378-.794)
Union by bridging of the cortical bone discontinuity by secondary lamellar bone	.443 (.191-.684)	.764 (.590-.884)	.939 (.882-.972)
Smoothing of the callus outline	.510 (.118-.838)	.348 (.013-.715)	.838(.652-.942)
Features specific for amputations⁴			
Visibility of cut marks on the amputation surface	1.000 ²	.733 (.409-.924)	0.000
Start of 'capping' of the medullary cavity.	1.000 ²	1.000 ²	1.000 ²
Complete closure of the medullary cavity	1.000 ²	.857 (.350-.996)	1.000 ²

Abbreviations: ICC=Intraclass Correlation Coefficient. CI=Confidence Interval. NA=Not Applicable.

¹Haematoxylin stained, according to De Boer et al. (2011).

² An ICC of 1.000 indicated no difference in observation between the examiners.

³ N=22.

⁴N=9.

Discussion

The results show that a considerable amount of healing features are still reliably detectable in dry bone tissue. Throughout the results, features indicating the same level of healing were in agreement with each other, supporting the statement that healing happens in an orderly, sequential fashion (e.g. Vigorita, 2009). The results will now be discussed in the time sequence in which they are reported to appear during the healing process (Barber 1929, 1930, 1934; Maat, 2008; Maat and Huls, 2010). This sequence is also described in Tables 2 and 5.

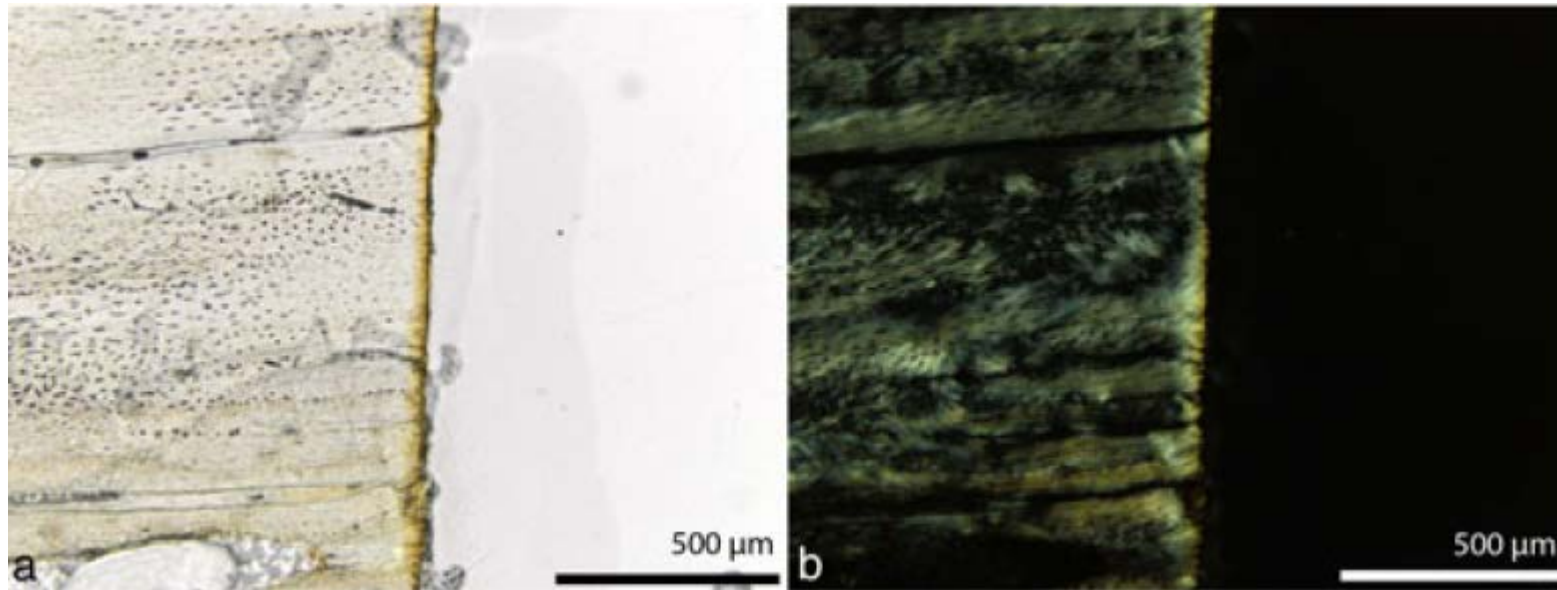


Figure 1. Micrographs of the frayed lesion margin of an amputated femur (S38.2). Undecalcified and unstained section. Bar indicates scale. Figure 1a) The cutting margin at the amputation end shows a frayed, brush-like appearance due to the fanning of bone lamellae. The yellow discolouring at the margin is caused by taphonomical processes. Figure 1b) Same section as 1a, now viewed with polarized light. The use of polarized light clearly enhances the visibility of the frayed margin.

Frayed bone lamellae at the lesion margins are reported to only be observable within the first 48 hours after injury. Due to the morphological character and dimensions of this feature, it could only be viewed by histological analyses. The use of histochemical staining did not affect the consistency of the detection. However, it was noted that the use of polarized light dramatically enhanced the visibility of frayed margins (Fig. 1)

Table 4. Intraclass Correlation Coefficients for healing features from histology

Healing feature	Unstained histology ICC (95% CI)	Stained histology ¹ ICC (95% CI)
Frayed bone lamellae at the lesion margins	.881 (.797-.936)	.763 (.620-.868)
Howship's lacunae at the lesion cleft	.700 (.533-.828)	.575 (.376-.745)
Howship's lacunae at the periosteal surface	.814 (.695-.989)	.599 (.405-.762)
Howship's lacunae at the endosteal surface	.903 (.832-.948)	.503 (.290-.695)
Cortical cutting and closing cones oriented towards the lesion	.965 (.922-.977)	.577 (.376-.747)
Remodeling of endosteal callus into secondary lamellar bone	.491 (.205-.742)	1.000 ²
Remodeling of periosteal callus into secondary lamellar bone	.242 (-.099-.627)	1.000 ²
Quiescent histomorphological appearance, indicating ended healing	1.000 ²	.741 (.583-.856)

Abbreviations: ICC=Intraclass Correlation Coefficient. CI=Confidence Interval.

¹Haematoxylin stained, according to De Boer et al. (2011).

² An ICC of 1.000 indicates no difference in observation between the examiners.

After four to seven days, lesion margins will start to become eroded by osteoclasts. Their activity is indicated by the presence of *Howship's lacunae*. These are only visible on a microscopic level. The use of histochemical staining impeded interobserver agreement. This might be due to confusion in microscopic image interpretation from the histotechnique of section surface staining. This leaves deeper situated tissue within the section unstained.

Osteoclastic activity on the lesion margins results in a *smoothing of the lesion margins*, at the earliest reported to be visible after four days. Good interobserver agreement was obtained irrespective of section staining. The unsatisfactory agreement in case of radiological analysis might be explained by difference in magnification and resolution (ICC of 0.416).

Due to a combination of taphonomic processes and excavation tissue damage, the next step in healing sequence, the formation of *bone spiculae between the lesion margins* (becoming visible after four to seven days) can not be found in dry bone specimens.

It was expected that by natural *absorption of cortical bone adjacent to the lesion margins*, margins would appear less opaque (see Table 2). However, this feature did not perform well in terms of interobserver agreement (ICC of 0.275). This might be explained by the difficulty to differentiate between antemortem healing changes and postmortem taphonomic alterations of the cortex.

After initial osteogenesis in the form of bone spiculae, callus formation starts both on the endosteal and periosteal aspect of the fractured bone. Minor *periosteal osteogenesis* (callus formation, visible after seven days) usually starts *at some distance* from the lesion site (Maat, pers. comm.) i.e. in the 'corner' where the periosteum is being lifted from the bone by the subperiosteal hematoma, resulting in an appearance similar to the radiological 'Codman's triangle' visible in osteosarcomas. From there it progresses

towards and unites with callus formation at the lesion site. Since this phenomenon only exists for a short period of time, it was unfortunately not observed in our sample. As a result, we examined periosteal callus at some distance as a part of the callus formation at the lesion site. This most likely caused the borderline interobserver agreement of the feature (ICC of 0.678 and stained 0.649). However, it is expected that if cases of early periosteal callus formation had been included in our collection, this could very well have shown to be consistently detectable.

Endosteal osteogenesis (callus formation) may start after seven days, and is usually *clearly visible* after ten to twelve days. It was consistently detected in both stained and unstained histological sections as well as during radiological analysis. In addition, we analyzed whether endosteally situated callus, like periosteal callus, also started at some distance from the site of lesion. Related Intraclass Correlation Coefficients were, however, low with broad 95% Confidence Intervals, both histologically (unstained ICC of 0.625 and stained ICC of 0.393) and radiologically (ICC of 0.345). This is probably due to the difficulty to differentiate between early endosteal callus formation and the naturally present surrounding cancellous bone.

As healing progresses, *local osteoporosis of the cortex* may be observable. This is usually not visible before twelve days. Osteoporosis within our sample was only consistently detected in stained and unstained histological sections, and not during radiological investigation (ICC of 0.341). The latter might be due to differences in technical resolution and magnification, resulting in more debatable findings in plain radiographs. This seems to especially hold true for early stages of local osteoporosis. In advanced phases, local osteoporosis becomes clearly visible on plain radiographs. See Figure 7.

As new bone formation progresses, the *margin of the lesion appears more sclerotic* (after 12-20 days, see Tab. 2). The related ICC, however, did not present substantial interobserver agreement (ICC of 0.421). As in the case of *local osteoporosis of the cortex*, this may be caused by differences in resolution and magnification.

In amputations, the presence of *cut marks* can be seen up till about 13 days after the traumatic event (see Table 2). This feature was only consistently reported in unstained and stained histological analysis, and was not consistently detectable with radiography (ICC of 0.000).

As stated earlier, loose microscopic *bone tissue spiculae* are undetectable due to postmortem decomposition. The same holds for the *fields of calcified cartilage* that only will be seen in fresh material after fourteen days.

After 14 days, the newly formed endosteal and periosteal callus starts its *transition from primary woven bone into secondary lamellar bone*. The histological detectability hereof was primarily analyzed with the use of polarized light, both in stained and unstained sections. However, our results suggest that staining increased consistent detection above the 0.6 threshold (endosteal: ICC of 0.491 vs. 1.000 and periosteal: ICC of 0.242 vs. 1.000). The phenomenon of improved visibility of separate bone lamellae by the use of haematoxylin was noted before by De Boer *et al.* (2010, 2011). The improvement in the ICC between stained and unstained sections may therefore be the result of a cumulative effect of staining and polarized light.

The remodeling process is accompanied by an increased number of *cortical cutting and closing cones*, observable two to three weeks after injury. Our results suggest a better

detectability in unstained sections (ICC of 0.965) if compared to stained sections (ICC of 0.577). As cortical cutting and closing cones are recognized by their characteristic two end conical shape with Howship's lacunae at their 'cutting' end, the previously noted negative effect of staining on the visibility on Howship's lacunae might have hampered detectability.

As remodeling progresses, *the endosteal callus becomes indistinguishable from the cancellous bone in the medullary cavity* (first visible after seventeen days). In radiological analysis, this was consistently detected. On a microscopic level, interobserver agreement was much higher in unstained than in stained sections (ICC of 0.845 vs. 0.370). This might be due to the above discussed confusing effect that histochemical staining may have on the visibility of overall bone tissue architecture.

According to Table 2, *periosteal callus becomes clearly visible* after about 15 days, observable both in stained and unstained histology, and radiological analysis. As callus formation progresses, the cortical defect in fractures is eventually bridged by callus after 21-28 days. This *union by bridging of the cortical bone discontinuity* was consistently detected in both (un)stained histological and radiological analyses.

Subsequently, the *periosteal callus becomes firmly attached (inseparable) to the cortex*. This is observable after six weeks and was only consistently detected in histological analysis, irrespective of the use of staining. Due to the earlier mentioned low resolution and magnification in plain radiographic images the ICC was very low (ICC of 0.015). The *smoothing of the callus outline* in fractures (after two to three months) was only consistently detected during radiological investigation (ICC of unstained 0.510 and stained 0.348 vs. radiology 0.838). The low magnification of routine radiographs now proved to be in favor of tissue overview if compared to histology.

In amputations, healing eventually progresses towards the *start of 'capping' of the medullary cavity* and the eventual *complete 'capping'* thereof. This was consistently detected in unstained and stained sections, as well as in radiological analysis. In fractures, healing eventually subsides, leaving a quiescent histomorphological appearance after 1-2 years. Both stained and unstained sections proved to be consistent.

The authors used interobserver agreement, assessed by means of Intraclass Correlation Coefficient (ICC) calculation, as an indicator for the consistency in detection of a healing feature. Cohen's Kappa is the most used statistical calculation for assessing interobserver agreement, but for comparisons between more than two examiners, ICC is regarded superior (Berk, 1979). The Intraclass Correlation Coefficient is defined as the proportion of true variance relative to total variance. In other words, a high ICC indicates that the method of analysis does not add variance to the total variance between subjects. Since calculation of the ICC uses total sample variation, its value is sensitive to the extensiveness of values in the sample. As a result, calculated ICC values are only 'reliable' in a heterogeneous population. As this research uses bone material with sufficient variability between healing phases, interobserver agreement on the presence of a parameter can reliably be calculated. When the Intraclass Correlation Coefficient is used as an indicator for consistency in observation, its calculated degree of agreement does not clarify whether a feature is detectable or undetectable. It only expressed the degree in consistency between examiners with respect to the detection of healing features.

We are aware of the limited sample size with regard to the number of amputations. Amputations are not frequently found in archaeological populations, and if so, not in

varying phases of healing. Nevertheless, since fractures and amputations generally share a similar healing process (Barber, 1930), it is believed that the combined assembly allows for meaningful interpretation. For those features in which logical inferences resulted in a limited number of examined specimens (e.g. complete closure of the medullary cavity in amputations), Intraclass Correlation Coefficient must be interpreted with caution, due to sample homogeneity.

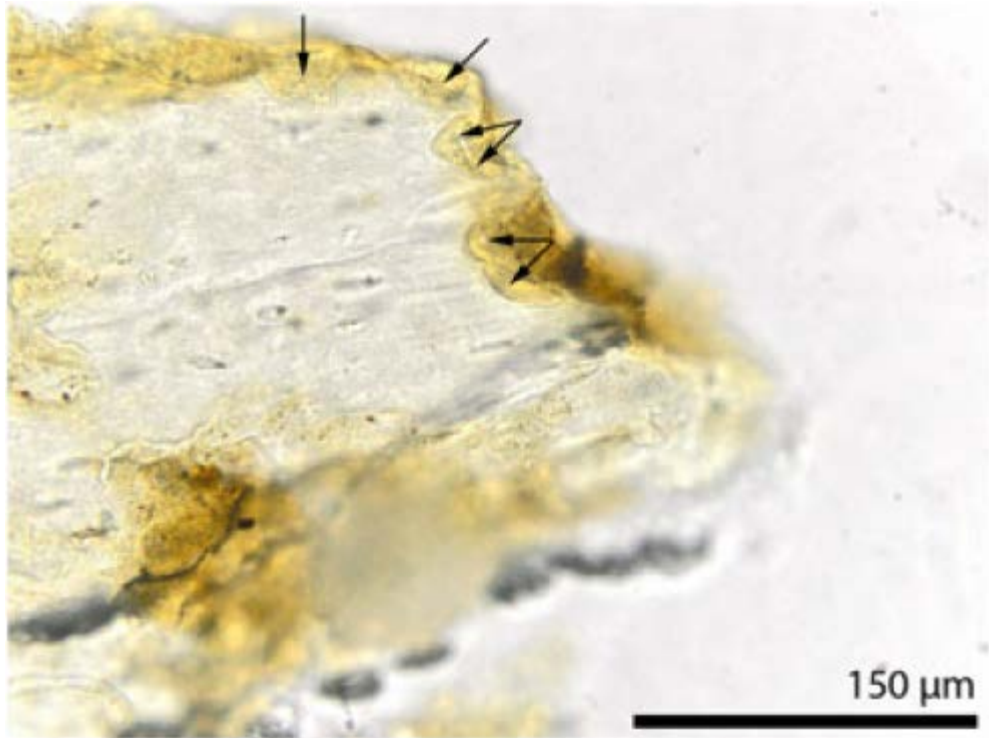


Figure 2. The fracture margin of a third metacarpal (N38.2) showing Howship's lacunae as numerous bite-like indentations (arrows). They are caused by resorption of bone tissue by osteoclasts. Undecalcified and unstained section. Bright light. Bar indicates scale.

Overall, our results suggest that not every healing feature as described by Barber (1929, 1930, 1934), Maat (2008) and Maat and Huls (2010) was consistently detected. Nevertheless the results from this study suggest that if only those with substantial interobserver agreement are used, a fair estimation of the minimal and maximal time lapsed after an injury can still be made. This is a substantial improvement in diagnosis if compared to conclusions such as 'healing' or 'healed'. For those who do not routinely 'date' fractures or amputations, a table was made showing only the consistently detected features together with its modality (Table 5). Furthermore, some reference figures are given (Figs. 1-7).

We recommend using plain radiographic and histological analysis. Histology yields the best results if both unstained and haematoxylin stained sections are used, in combination with polarized light. And, as usual, the value of negative observations is limited, in contrast to positive observations. Time intervals should be adjusted to specific conditions (e.g. shortened in case of children (Maat, 2008; Maat and Huls, 2010)). It goes without

Table 5. Consistently detected healing features visible in dry bone material

Healing feature	Time interval	Unstained histology	Stained histology ¹	Plain radiography
<ul style="list-style-type: none"> • Frayed bone lamellae at the lesion margins • First Howship's lacunae at the lesion margins • Smoothing of the lesions margins • Start of periosteal callus formation, distant from the lesion margins, separable from the cortex. 	Before 48 hours After 4-7 days After 4-7 days After 7 days	x x x x	x x x	
<ul style="list-style-type: none"> • Endosteal callus formation clearly visible • Osteoporotic appearance of the cortex • Start of the transition of primary woven bone into secondary lamellar bone 	After 10-12 days After 12 days After 14 days	x x 	x x x	x x
<ul style="list-style-type: none"> • Cortical cutting and closing cones orientated towards the lesion • Clearly visible periosteally situated callus • Endosteal callus becomes indistinguishable from the cancellous bone in the marrow cavity • Periosteal callus becomes firmly attached (inseparable) to the cortex 	After 14-21 days After 15 days After 17 days After 6 weeks	x x x x	 x x x	 x x
<i>Features specific for fractures</i>				
<ul style="list-style-type: none"> • Union by bridging of the cortical bone discontinuity <ul style="list-style-type: none"> ○ by primary woven bone ○ by secondary lamellar bone • Smoothing of the callus outline • After adequate immobilization: quiescent appearance indicating subsided healing. 	After 21-28 days After 2-3 months After 1-2 years	x x x	x x x x	x x
<i>Features specific for amputations</i>				
<ul style="list-style-type: none"> • Visibility of cut marks on the amputation surface • Start of 'capping' of the medullary cavity • Complete capping of the medullary cavity 	Before 13 days 'After not many weeks' 'After several months'	x x x	x x x	 x x

¹Haematoxylin stained, according to De Boer et al. (2011).

saying that our approach stays open for improvement and reliability will increase with experience.

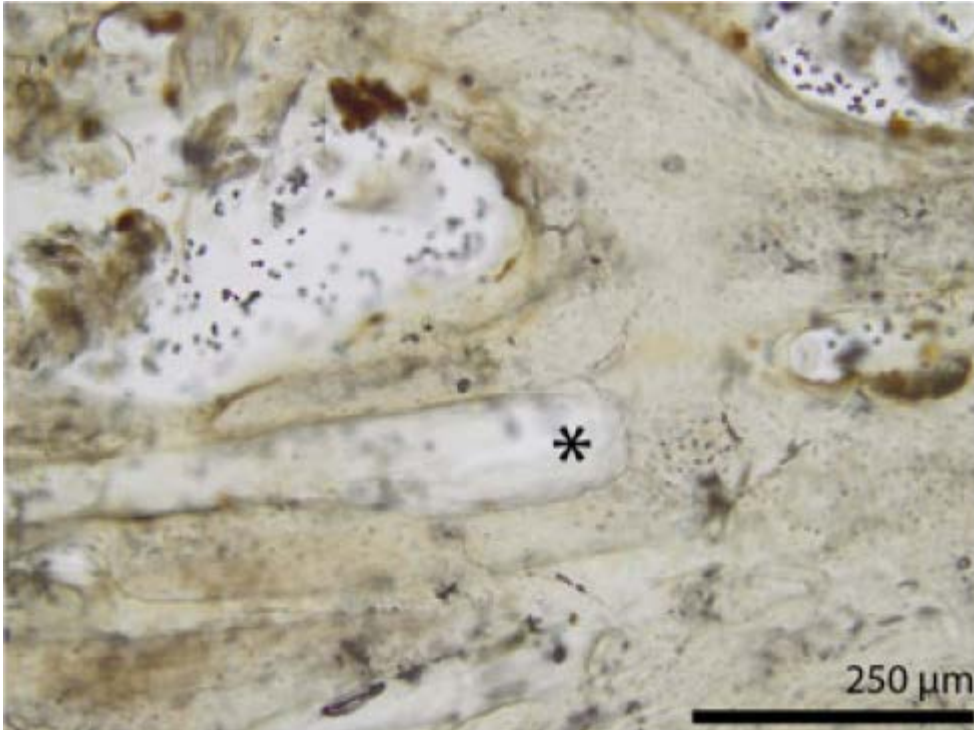


Figure 3. Micrograph taken near the fracture site of a fractured radius (N38.3). In the centre, a ‘cutting cone’ running/drilling from left to right is indicated (asterisk). The cutting cone is characterized by Howship’s lacunae. The closing cone is situated to the left, outside the field of photography. Undecalcified, unstained section. Bright light. Bar indicates scale.

Conclusion

By using complementary radiological and (un)stained histological investigation methods, a differentiation can be made between features that indicate various stages of the healing process after trauma as may be observed in human dry bone material. The consistency in the detection of healing features indicate that the bone healing process can be used to estimate the posttraumatic time interval of fractures and amputations.

Acknowledgements

We are indebted to the Leiden University Fund (LUF)/Van Trigt and the South Africa Netherlands research Programme for Alternatives in Development (SANPAD) for partial funding. We also thank the Department of Radiology of the LUMC and Ron Wolterbeek of the Department of Medical Statistics of the LUMC. We are greatly indebted to Dr David Morris of the McGregor Museum in Kimberley, South Africa, for allowing us to use the Gladstone material.

Conflict of interest

The authors declare no conflict of interest.

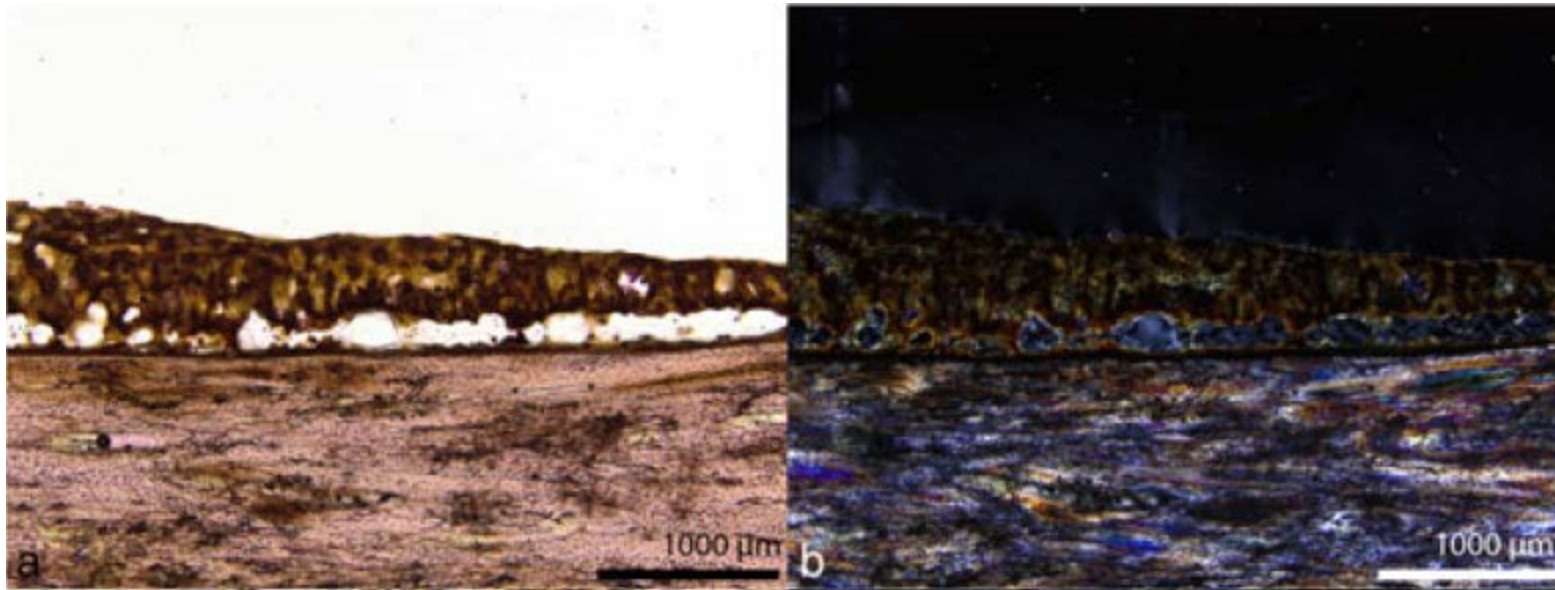


Figure 4. Micrographs of so-called 'separable periosteal callus' in a fractured third metacarpal (N.38.2). Undecalcified section, stained with haematoxylin. Bar indicates scale. Figure 4a) Section viewed with bright light. The separable periosteal callus is only connected to the periosteal aspect of the cortex by small pillars of bone tissue. The sloping aspect of the callus illustrates the build-up of callus towards the fracture site. Figure 4b) Same section as shown in Figure 4a, now viewed with polarized light. Extensive taphonomic alteration of the periosteal callus hampers the visibility of the microarchitecture of the callus. The callus in this healing phase constitutes mainly of primary woven bone, in contrast to the secondary lamellar bone of the underlying cortex.

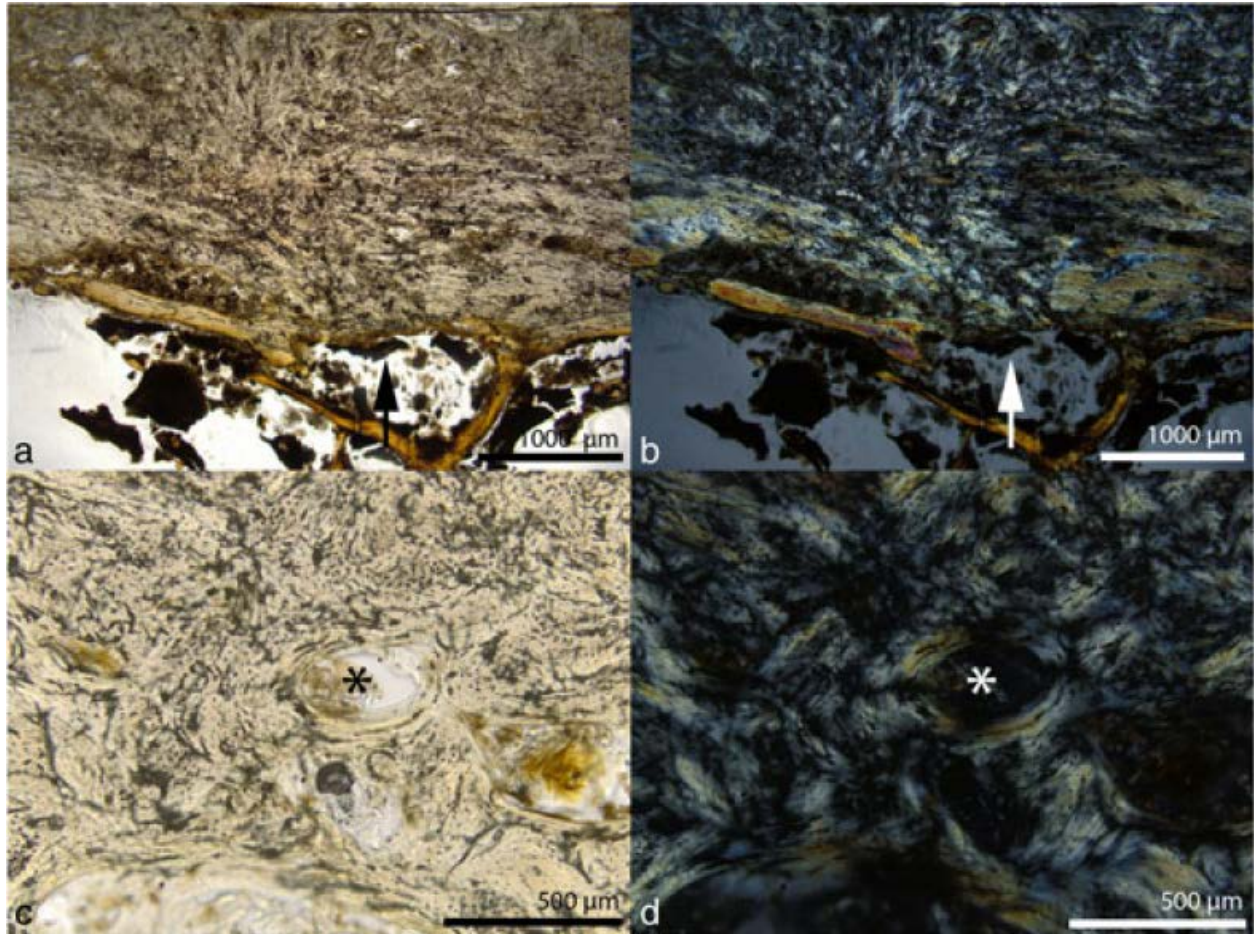


Figure 5. Micrographs showing the remodeling of callus in a fractured radius (N38.3). Undecalcified, unstained section. Bar indicates scale. Figure 5a) Section viewed with bright light. Overall, the callus has a disorganized appearance and consists mainly of primary woven bone. The lesion site is indicated by an arrow. Figure 5b) Same section as shown in Figure 5a, now viewed with polarized light. The use of polarized light enhances the random orientation of the primary woven bone fibers. Also, the discontinuity of the cortex at the lesion site (arrow) is enhanced by polarized light. Figure 5c) Detail of the callus as shown in 5a and 5b. Viewed with bright light. A higher magnification shows one of the Haversian canals (asterisk), indicating that advanced remodeling of the callus has started. Figure 5d) Same section as shown in Figure 5c, viewed with polarized light. The detectability of Haversian systems, organized around a Haversian canal (asterisk), becomes indisputed by the use of polarized light.



Figure 6. Radiographs of remodeled calluses. Top: The X-ray of a fractured radius (N.38.3) shows both an endosteally and a periosteally situated callus. The periosteal callus has a smoothed outline. Continuity of the cortex is restored, although its bone density at the lesion site is still decreased. Below: This X-ray of a fractured ulna (N74.4) shows a smoothed periosteally situated callus. The continuity of the cortex is almost totally restored and is slightly less radiodense at the fracture site. The internal callus is almost indistinguishable from the surrounding cancellous bone of the marrow cavity, indicating advanced remodeling.

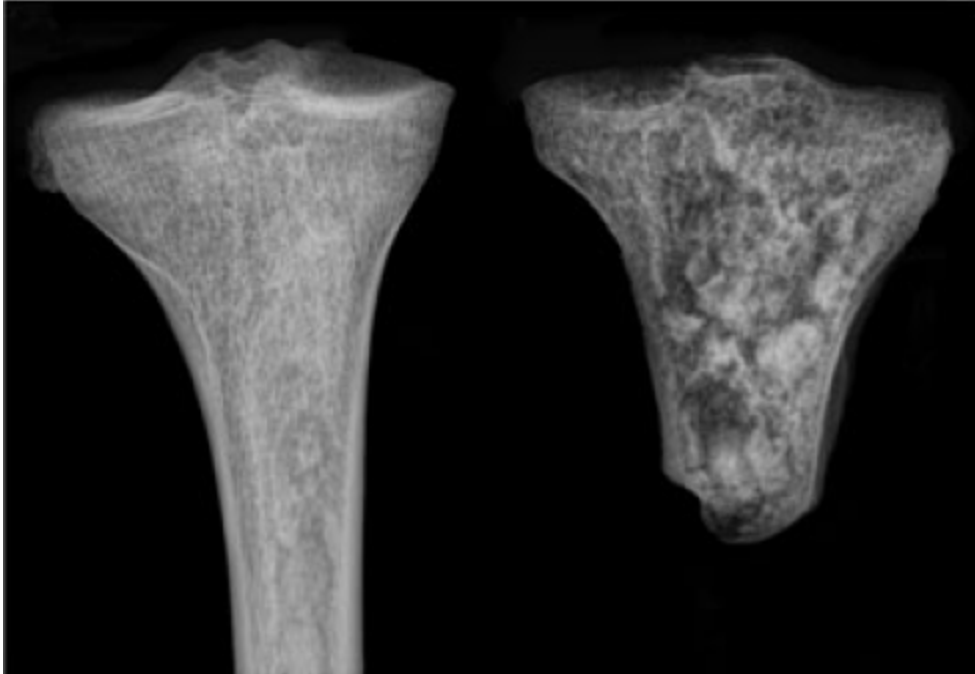


Figure 7. Radiograph of an amputated tibia (N34.3). When compared to its contralateral control, The amputated stump shows diminished density of the cancellous bone and a thinned cortex. This indicates osteoporosis due to disuse. The medullary cavity at the amputation end is almost closed by new bone formation, indicating advanced capping. The mottled appearance of the tibial stump is partly due to dirt.

Literature Cited

- Alvrus A. 1999. Fracture patterns among the Nubians of Semna South, Sudanese Nubia. *International Journal of Osteoarchaeology* **9** (6): 417-429.
- Anderson T. 2002. Healed trauma in an early Bronze Age human skeleton from Buckinghamshire, England. *International Journal of Osteoarchaeology* **12** (3): 220. DOI: 10.1002/oa.599
- Aufderheide AC, Rodríguez-Martin C. 1998. *The Cambridge Encyclopedia of Human Palaeopathology*. Cambridge: Cambridge University Press.
- Barber CG. 1929. Immediate and eventual features of healing in amputated bones. *Annals of Surgery* **90** (6): 985-992
- Barber CG. 1930. The detailed changes characteristic of healing bone in amputation stumps. *Journal of Bone and Joint Surgery* **12**: 353-359.
- Barber CG. 1934. Ultimate anatomical modifications in amputation stumps. *Journal of Bone and Joint Surgery* **16** (2): 394-400.
- Berk RA. 1979. Generalizability of behavioral observations: A clarification of interobserver agreement and interobserver reliability. *American Journal of Mental Retardation* **83**(5):460-472.
- Berryman HE, Haun SJ. 1996. Applying forensic techniques to interpret cranial fracture patterns in an archaeological specimen. *International Journal of Osteoarchaeology* **6**: 2–9.
- Brickley M. 2006. Rib fractures in the archaeological record: a useful source of sociocultural information? *International Journal of Osteoarchaeology* **16** (1): 61-75. DOI: 10.1002/oa.809
- Cattaneo C, Andreola S, Marinelli E, Poppa P, Porta D, Grandi M. 2010. The detection of microscopic markers of hemorrhaging and wound age on dry bone: a pilot study. *American Journal of Forensic Medicine & Pathology* **31** (1): 22.
- De Boer HH, Aarents MJ, Maat, GJR. 2010. Staining ground sections of natural dry bone tissue for microscopy. *International Journal of Osteoarchaeology* (in press) DOI: 10.1002/oa.1208
- De Boer HH, Aarents MJ, Maat, GJR. 2011. Manual for the preparation and staining of embedded natural dry bone tissue sections for microscopy. *International Journal of Osteoarchaeology* (in press) DOI 10.1002/oa.1242
- Djurić MP. 2006. Fractures in late medieval skeletal populations from Serbia. *American journal of Physical Anthropology* **130** (2): 167-178 DOI: 10.1002/ajpa.20270
- Frost HM. 1989. The biology of fracture healing: an overview for clinicians. Part I. *Clinical Orthopedics and Related Research* **248**: 283-293.
- Frost HM 1989. The biology of fracture healing: an overview for clinicians. Part II. *Clinical Orthopedics and Related Research* **248**: 294-309

Grauer AL , Roberts CA. 1996. Paleoepidemiology, healing, and possible treatment of trauma in the medieval cemetery population of St. Helen-on-the-Walls, York, England. *American Journal of Physical Anthropology* **100** (4): 531-544.

Gordon CG, Buikstra JE. 1981. Soil pH, bone preservation, and sampling bias at mortuary sites. *American Antiquity* 46: 566–571.

Holt BM, Fornaciari G, Formicola V. 2002. Bone remodelling following a lower leg fracture in the 11, 000-year-old hunter-gatherer from Vado all' Arancio(Italy). *International Journal of Osteoarchaeology* **12** (6): 402. DOI: 10.1002/oa.639

Judd MA, Roberts CA. 1999. Fracture trauma in a medieval British farming village. *American Journal of Physical Anthropology* **109** (2): 229-243.

Krogman WM, Iscan MY. 1986. *The human skeleton in forensic medicine*. Springfield, USA: Charles C. Thomas Publisher.

Landis JR, Koch GG. 1977. The measurement of observer agreement for categorical data. *Biometrics* **33** (1): 159-174.

Lovell NC. 1997. Trauma analysis in paleopathology. *Yearbook of Physical Anthropology*. **104**: 139-170.

Maat G.J.R. 1981. Human remains at the Dutch whaling stations at Spitsbergen, a physical anthropological report., 153-201. Groningen: University of Groningen.

Maat GJR. 2008. Case study 5.3: Dating of fractures in human dry bone tissue - the Berisha case. In *Skeletal trauma*. Kimmerle EH and Baraybar JP (eds). Taylor & Francis Group: Boca Raton, FL; 245-254

Maat GJR, Huls N. 2010. Histological fracture dating of fresh and dried bone. In *Forensic Aspects of Pediatric Fractures*. Bilo RAC, Robben SGF and Van Rijn R (eds.). Springer-Verlag: Berlin - Heidelberg; 194-201

Mays SA. 1996. Healed limb amputations in human osteoarchaeology and their causes: a case study from Ipswich, UK. *International Journal of Osteoarchaeology* **6** (1): 101-113.

Van der Merwe AE, Steyn M, l'Abbé EN. 2009. Trauma and amputations in 19th century miners from Kimberley, South Africa. *International Journal of Osteoarchaeology*. (in press)
DOI:10.1002/oa1035

Mitchell PD. 2006. Trauma in the Crusader period city of Caesarea: a major port in the medieval eastern Mediterranean. *International Journal of Osteoarchaeology* **16** (6): 493-505.
DOI: 10.1002/oa.853

Nakai M, Koji I, Sinsuke H. 2001. Healed bone fractures in a Jomon skeletal population from the Yoshigo shell mound, Aichi Prefecture, Japan. *International Journal of Osteoarchaeology* **9** (2): 77-82.

Oehmichen M. 2004. Vitality and time course of wounds. *Forensic Science International* **144** (2-3): 221-231. DOI: 10.1016/j.forsciint.2004.04.057

Ortner DJ. 2003. *Identification of pathological conditions in human skeletal remains*. Academic Press: San Diego.

Quatrehomme,G.; Iscan,M.Y. 1997. Postmortem skeletal lesions. *Forensic Science International* **89** (3): 155-165.

Redfern R. 2009. A regional examination of surgery and fracture treatment in Iron Age and Roman Britain. *International journal of osteoarchaeology* **20** (4): 443-471.
DOI: 10.1002/oa.1067

Rodríguez-Martin C. 2006. Identification and differential diagnosis of traumatic lesions of the skeleton. In: *Forensic Anthropology and Medicine: Complementary Sciences From Recovery to Cause of Death*. Schmitt A, Cunha E and Pinheiro J (eds).: 197-221. Totowa, NJ: Humana Press.

Todd TW, Iler DH. 1927. The phenomena of early stages in bone repair. *Annals of Surgery* **86** (5): 715-736.

Todd TW, Barber CG. 1934. The extend of skeletal change after amputation. *Journal of Bone and Joint Surgery* **16** (1): 53-64.

Tosounidis T, Kontakis G ,Nikolaou V, Papathanassopoulos A, Giannoudis PV. 2009. Fracture healing and bone repair: an update. *Trauma* **11** (3): 145-156.

Vigorita VJ. 2009. *Orthopaedic pathology*. Lippincott, Williams and Wilkins: Philadelphia, New York, Baltimore.

Wieberg DA and Wescott DJ. (2008), Estimating the timing of long bone fractures: correlation between the postmortem interval, bone moisture content, and blunt force trauma fracture characteristics. *Journal of Forensic Sciences* **53**: 1028–1034.

Wheatley BP. 2008. Perimortem or Postmortem Bone Fractures? An Experimental Study of Fracture Patterns in Deer Femora*. *Journal of Forensic Sciences* **53** (1): 69.
DOI: 10.1111/j.1556-4029.2008.00593.x